

## YSO disk structure and planetary signatures

Nuria Calvet

*Harvard-Smithsonian Center for Astrophysics, 60 Garden St., MS 42,  
Cambridge, MA -2138*

Paola D'Alessio

*Instituto de Astronomía, UNAM, Ap.P. 70-264, 04510 México D.F.*

### **Abstract.**

Detailed radial/vertical structure modeling of observations of disks around Young Stellar Objects (YSOs) can provide information on the physical conditions and on the characteristics of the gas and dust in their interiors. We describe recent results of self-consistent modeling of spectral energy distributions, optical and infrared images, and millimeter fluxes of YSOs. We discuss observations and interpretations of the initial stages of planet formation, including indications of dust growth and settling in disks around young stars. We also discuss how the unprecedented resolution and sensitivity of ALMA may help us study the interior of the innermost disks, a region inaccessible with present day instrumentation, and witness the very first stages of planet formation.

### **1. Introduction**

Since the late 1970s, it was known that the low mass pre-main sequence T Tauri stars were surrounded by disks. For instance, the lack of correlation between the (near infrared) excess and the extinction had led to the suggestion that the cool material producing the excess was located in a geometrically flat configuration (Cohen & Kuhl 1979). However, it was not until the first *IRAS* observations of TTS appeared that the large mid and far infrared excesses were attributed to accretion disks (Rucinski 1985), in agreement with the original suggestion of Lynden-Bell & Pringle (1974). Masses and radii for these disks were estimated from submillimeter and millimeter observations around the late 1980's. The indirect inference for disks from all these observations was dramatically confirmed in this decade, when disks around young stars have been directly imaged by instruments on board of *HTS*. Disks are seen against the bright background of the Orion nebula as silhouettes (McCaughrean & O'Dell 1996; McCaughrean et al. 1998; Stauffer et al. 1999), and in the favorable edge-on situations, where the direct light from the star is blocked by the disks, so the faint glow of stellar light scattered by dust grains on the disk surface can be seen. A number of cases have been presented so far; the best known and analyzed include HH30 (Burrows et al. 1996) and HK Tau/c (Stapelfeldt et al 1998). These disks are the predecessor of planetary systems.

T Tauri disks are composed of gas and dust. The mass in the disk is of the order of a few  $0.01 M_{\odot}$ , and matter is still accreting onto the star. On the other extreme, in disks with planetary systems, most of the mass is on the planets, a few  $0.001 M_{\odot}$ , and only small amount of dust ( $\ll 10^{-6} M_{\odot}$ ) remains. The transition between these two stages is of utmost interest. What are the processes that lead to planet formation and in which timescales?

In this contribution, we argue that the first signs of the transition to planetary disks appear in the inner disk, within a few AU from the star, and then when this transition starts, it happens very fast. We will review evidences provided by two groups of different ages, 1-2 Myr and 10 Myr. We then will argue that present and future observations in the optical and infrared cannot tell us what is happening near the midplane of the inner regions of the gas and dust disks characterizing the initial stages before the transition. Only ALMA, in the highest resolution configuration, will allow us to scrutinize the innermost disk and to obtain information on the processes occurring to the dust in these regions leading to the formation of planets.

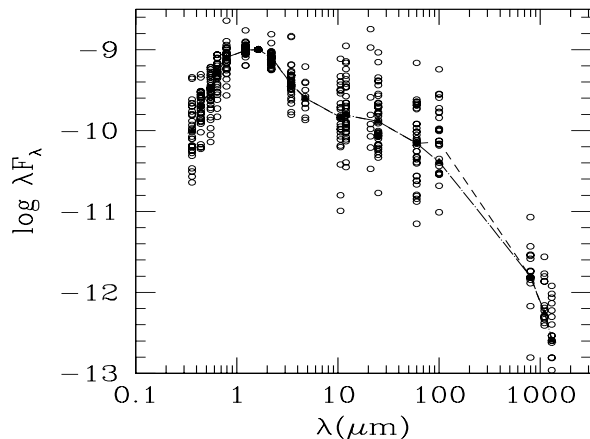


Fig. 1. Fluxes of classical T Tauri stars in Taurus-Auriga. From D'Alessio et al. (1999b.) Fluxes are normalized at H. The solid line is the mean SED constructed from these data, including upper limits at  $100\mu\text{m}$ . The dashed line does not include these upper limits.

## 2. Indications of dust evolution

Figure 1 shows fluxes for all classical T Tauri stars (CTTS) in Taurus-Auriga, scaled at H (D'Alessio et al. 1999b). The large infrared excesses due to disk emission are apparent. Disk emission depends on the temperature of the disk, which in turn, is determined by the amount of heating. Two agents can heat the disk: viscous dissipation related to accretion, and stellar irradiation. For the typical values of the mass accretion rates in the disks around CTTS (Gullbring et al. 1997; Hartmann et al. 1998), irradiation from the central star plays a dominant role in the heating of the disk (Kenyon & Hartmann 1987, KH87;

D’Alessio et al. 1998, 1999a,b,c). Heating by irradiation will depend on the shape of the disk surface, since disks with flared surfaces can capture more stellar radiation than flat disks (KH87). In turn, the scale height of the disk, and therefore the height of the surface, depends on the disk temperature. A self-consistent stability analysis of irradiated disks for typical CTTS parameters indicates that a unique, stable solution for the surface exists, and corresponds to a flared surface (D’Alessio et al. 1999a). This means that disk emission will be determined essentially by how much energy comes into the disk, set by the star, and how much of this energy is actually absorbed and re-emitted by the disk, which depends on the dust in the disk.

Most stars in Taurus shown in Figure 1 have spectral types between K7 and M3, so they have similar amounts of stellar irradiation. The large dispersion observed in the SEDs must essentially be due then to differences in the dust properties in the disk, indicating that even though the stars have similar ages (1 - 2 Myr, Gomez et al. 1993), there is a large diversity in the conditions of the dust in these disks.

Figure 2 shows the SEDs for two “transition cases” in Taurus: DI Tau (Meyer et al. 1997) and V819 Tau (M. Meyer, personal communication). These stars are weak TTS, that is, they are not accreting mass onto the star. The indications of disk accretion, i.e., broad emission line profiles, UV excesses, which characterize CTTS are not present in these stars, nor are near-infrared excesses. However, mid-infrared and even millimeter flux excesses persists, indicating that remnants of the disk are still there. Some other transition cases may exist and remain to be discovered, but not in large numbers; the total number of transition cases may be less than 10, which when compared to the total number of TTS in Taurus,  $\sim 100$ , indicates that the loss of the disk happens fast. The actual processes causing disk dissipation are not well known, and binary companions may play a crucial role in clearing the disks; but in any event, the processes leading to disk dissipation occur in very short timescales, compared to the lifetime of a typical T Tauri star.

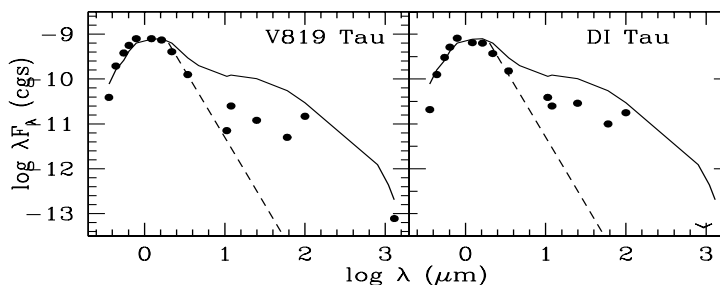


Fig. 2. SEDs of two “transition” T Tauri stars in Taurus: DI Tau (right) and V819 Tau (left) (data from Kenyon & Hartmann 1995). These are weak T Tauri stars, where accretion has already stopped, but still with mid and far infrared excesses. The median SED in Taurus (solid line) and photospheric fluxes (dashed line) are shown for comparison.

Figure 3 shows SEDs for stars in the TW Hya association, which has an estimated age of 10 Myr (Webb et al. 1999) from Jayawardhana et al. (1999). Although TW Hya itself has been known for many years (Herbig 1978; Rucinski & Krautter 1983; de la Reza et al. 1989) as an “isolated T Tauri star”, it is not until recently that this extremely interesting association has begun to be extensively studied. The main problem has been finding its members, since molecular gas is no longer associated with the association. Most of the members found are turning out to be weak TTS, but a few of them still show indications of disk emission, similar to the mean SED in Taurus in the mid and far-IR and in the millimeter (Figure 3). Again, in some cases, a deficit in the near-IR compared to longer wavelengths seem to be present.

The evidence provided by young stars in the two extremes of the temporal range where disks are expected to dissipate and planets to form ( $\sim 10$  Myr, Podosek & Cassen 1994) indicates that disks can last for a very long time, but once clearing starts, it occurs in very short time-scales. The first signs of disk clearing seem to appear in the near-IR, indicating that the higher temperature regions in the inner disk are the first to clear up. This is consistent with the evidence provided by debris disks; for instance, in the youngest debris disk known, around the A0 star HR 4796A,  $\sim 8$  Myr (Jayawardhana et al. 1998; Koerner et al. 1998), a possible member of the TW Hya association, disk emission is only apparent beyond 10 microns. The inner disk has been cleared out maybe by a planet or planets, consistent with the images in the mid-IR and in the near-IR from *HST* (Telesco et al. 1999; Schneider et al. 1999).

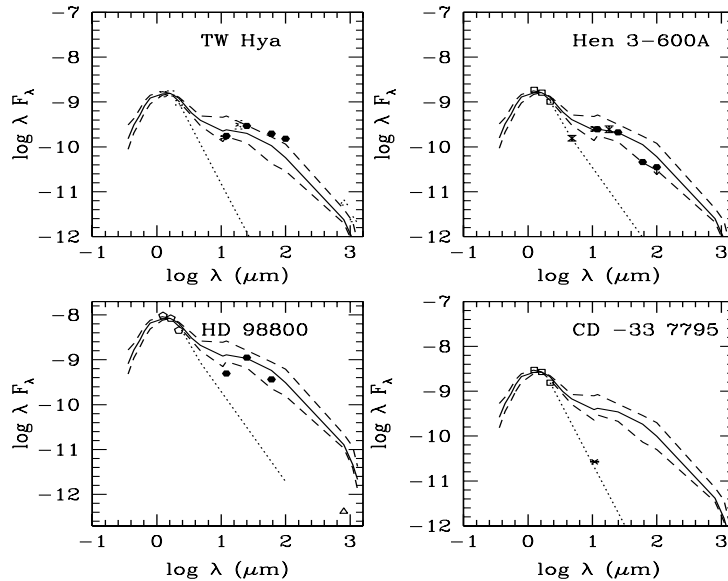


Fig. 3. SEDs of stars in the TW Hya association. From Jayawardhana et al. (1999). The solid curve is the median SED in Taurus, and the dashed lines indicate the quartiles. The dotted line indicates the photosphere.

The process of inner disk clearing must start with dust growth and settling towards the midplane. Eventually, a planet (or planets) forms in the disk, and

a gap is opened at the position of the planet; the inner disk is accreted onto the star, while a considerable fraction of the remaining mass of the disk goes into planet formation. Disks around CTTS must be in the very first stages of this sequence; once planets form and gaps appear, the evolution happens very fast, and it may prove difficult to find disks with gaps, still retaining the inner disk. It may bear more results to study the early phases, previous to planet formation, when the star still retains its original gas plus dust disk, searching for indication of dust coagulation and settling.

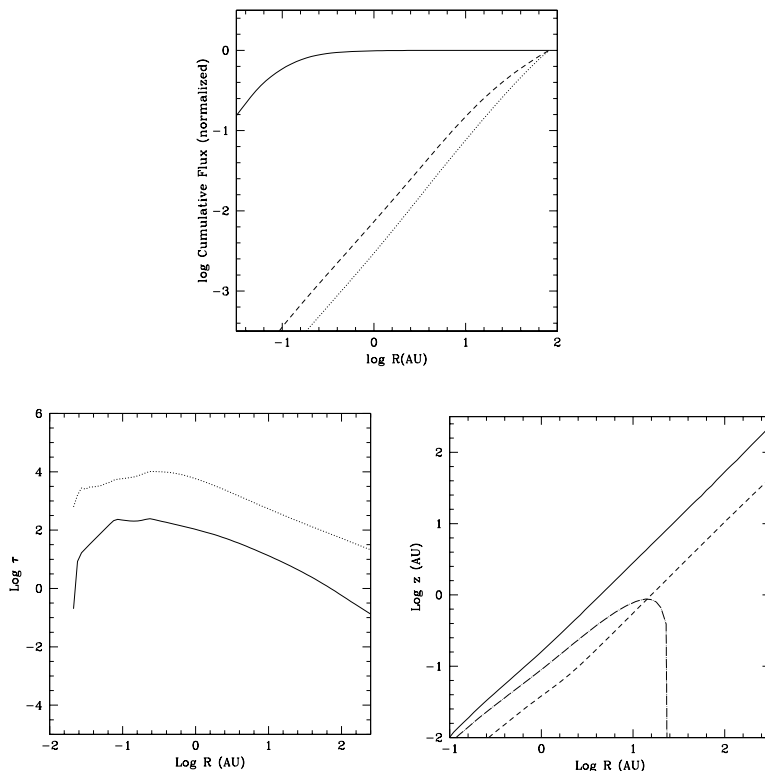


Fig. 4. Upper panel: (a) Disk cumulative flux as a function of radius at three wavelengths:  $10 \mu\text{m}$  (solid),  $0.5 \text{ mm}$  (dotted) and  $1 \text{ mm}$  (dashed). The disk model has typical parameters for CTTS: mass  $0.5 M_{\odot}$ , radius  $2 R_{\odot}$ , mass accretion rate  $10^{-8} M_{\odot} \text{ yr}^{-1}$ , and effective temperature  $4000\text{K}$ . Lower left: (b) Characteristic optical depths in the disk:  $\tau(1\mu\text{m})$ , where stellar radiation is absorbed (dotted);  $\tau_{Ross}$ , the optical depth at the local radiation (solid). The disk is optically thick to the stellar radiation even in the outer regions where it becomes optically thin (to its own radiation). Lower right: (c) Characteristic heights in the disk:  $z_s$ , surface where  $\tau(1\mu\text{m}) \sim 1$  (solid); the disk scale height (dashed);  $z_{phot}$ , surface where  $\tau_{Ross} \sim 1$  (defined where the disk is optically thick)(long dashes).

### 3. The Tauri disks

Self-consistent radial/vertical calculations of disk structure for typical CTTS parameters, including viscous and irradiation heating, have been carried out by D'Alessio et al. (1998, 1999b,c). These calculations show that the flux at  $\lambda \leq 10 \mu\text{m}$ , where the first indications of disk clearing appear, comes from the region inside a few AU of the disk. Figure 4a shows the cumulative flux at three wavelengths, normalized at the maximum, indicating that only in the millimeter range the whole disk is contributing to the flux.

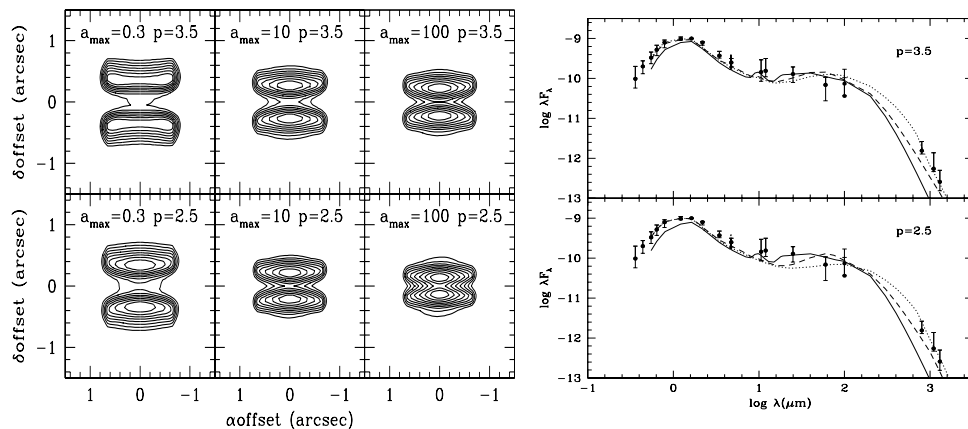


Fig. 5. Left: *HST* scattered light model images at  $0.8\mu\text{m}$  for edge-on disks, corresponding to dust well mixed with gas and different size distribution and maximum size (see text). Right: SEDs for models with images in the left size.  $a_{\text{max}} = 0.3\mu\text{m}$  (solid),  $10 \mu\text{m}$  (dashed), and  $100 \mu\text{m}$  (dotted). From D'Alessio et al. (1999c).

Figure 4b shows characteristic optical depths in the disk. The optical depth at  $\lambda \sim 1\mu\text{m}$ , at the peak of the stellar radiation, is always much larger than 1, since dust opacity is high at optical and near-IR wavelengths. In contrast, the Rosseland mean optical depth, which corresponds to the optical depth to the local radiation, falls below 1 beyond  $\sim 10$  AU. This means that the disk is thick to stellar radiation even when it is optically thin to the local radiation (for instance, in the outer disk.) This last property implies that the disk can efficiently capture stellar radiation up to a few hundred AU, of the order of the estimated radii of CTTS (Beckwith et al. 1990; Dutrey et al. 1996). It also implies that scattered light images of edge-on disks observed with *HST* should show the flared shape characteristic of the surface where stellar irradiation is being captured, as it is indeed the case. Figure 4c shows this surface,  $z_s$ , as well

as the scale height and  $z_{phot}$ , the height of the optically thick disk (obviously defined only in the region where the disk is thick).

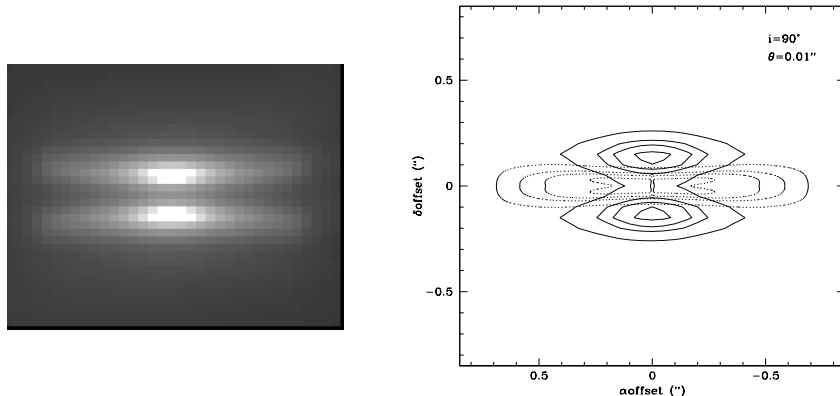


Fig. 6. Left: Model scattered light *HST* image at  $0.9 \text{ \AA}$  for typical CTTS parameters. Right: isocontours of image on left (solid), superimposed to disk emission observed with ALMA at  $0.9 \text{ mm}$  with  $0.01''$  resolution (dotted).

*HST* scattered light images and SEDs of CTTS may already be given indication of dust growth in the disk. Figure 5 shows calculations of images and SEDs for a mixture of astronomical silicates and graphite (Draine & Lee 1987, DL87), with a size distribution  $n(a) \propto a^{-p}$ , with  $p = 3.5$  (MRN, typical of interstellar medium dust, DL 87) and  $p = 2.5$  (indicating some degree of coagulation, Miyake & Nakagawa 1995). The minimum size of the dust is  $a_{min} = 0.005 \mu\text{m}$  (DL87) and the maximum size is  $a_{max} = 0.3 \mu\text{m}$  (DL87, ISM dust),  $10 \mu\text{m}$ , and  $100 \mu\text{m}$ , for fixed dust to gas ratio. As the maximum grain size increases, the opacity decreases in the optical and near-IR, as more of the dust is locked in bigger grains; at the same time, the opacity increases in the millimeter range. The effect of grain growth on scattered light images is shown in Figure 5, left. ISM dust produces images where the widths of the lanes separating the bright nebulae above and below the disk are of the order of  $\sim 100 \text{ AU}$  (at Taurus), which is larger than the width of the observed edge-on disks (D’Alessio et al. 1999b). The width of the lane decreases as  $a_{max}$  increases, as a result of the decreased opacity in the optical and the consequent lowering of the surface where  $\tau(1 \mu\text{m}) \sim 1$ , producing better matches to the observations. At the same time, mixtures with larger grains produce much better agreement between the typical CTTS disk model fluxes and the median Taurus SED (Figure 5, right).

#### 4. Scrutiny of the deep inner disk: only with ALMA

*HST* observations, even at  $\sim 0.05''$  resolution, can only probe the upper regions of the disk, because the CTTS disk is *always optically thick to optical and near-IR radiation*. Only submillimeter and millimeter observations can reach the mid-

plane of the disk. But present day interferometers can only give us a resolution of at most  $\sim 40$  AU at the closest star formation regions. This implies that we have no direct observations to constraint the detailed structure of the regions near the midplane in the inner disk regions. ALMA at the highest resolution,  $\sim 0.01''$ , will constitute the perfect complement to *HST* observations, allowing us to reach the true scale height of the disk. To illustrate this, Figure 6 compares typical CTTS model calculations for a scattered light *HST* edge-on disk image at  $0.9 \text{ \AA}$  and the corresponding ALMA image at  $0.9 \text{ mm}$  with  $0.01''$  resolution.

Moreover, with the highest ALMA resolution,  $0.01'' \sim 1.4 \text{ AU}$  at Taurus, we will be able to probe different heights at the innermost disk regions observing at different wavelengths. Figure 7, left, shows the heights in the disk where  $\tau \sim 1$  at different wavelengths. In the submillimeter range and beyond, the disk opacity is low enough to allow inspection of regions closer and closer to the midplane. These observations will allow us for the first time to *effectively map the inner disk structure*.

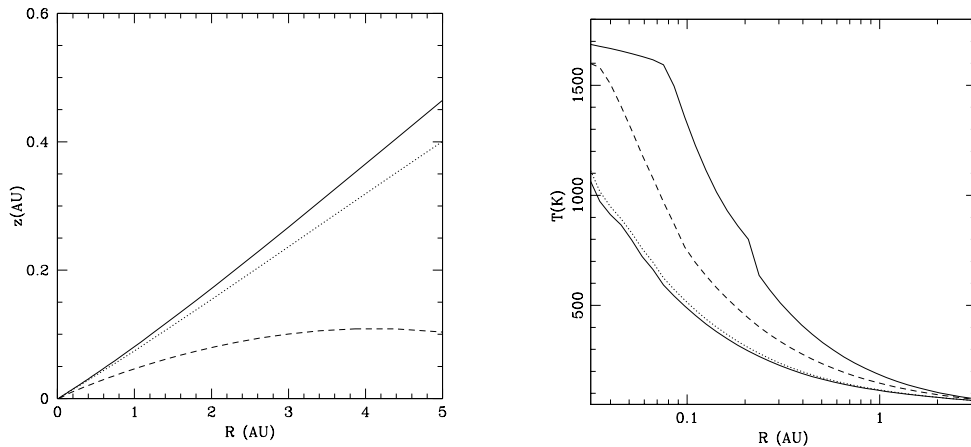


Fig. 7. Left: Height in AU at which the optical depth becomes 1 at given  $\lambda$ , i.e., height of formation of radiation at  $\lambda$ , for the case of gas and dust well mixed and  $a_{max} = 100 \mu\text{m}$ . Light solid:  $0.5 \mu\text{m}$ , dotted:  $0.5 \text{ mm}$ , dashed:  $1 \text{ mm}$ . Right: Brightness temperature at different  $\lambda$ , corresponding to heights in left. The heavy solid line is the midplane temperature.

The temperature in the inner disk,  $T(z, R)$  depends on local conditions. Using the diffusion approximation,  $dT/dz \propto \kappa F$ . The opacity  $\kappa$  will depend on the dust properties, type, size, and vertical distribution. The flux generated at each height,  $F$ , will depend on the local viscous generation of energy. Figure 7, right, shows the brightness temperature at several wavelengths, for the case of dust with  $a_{max} = 100 \mu\text{m}$ , well mixed with gas, and viscous heating at each height. Because of the large opacity, the temperature in the mid-plane is much higher than the surface temperature. Brightness temperatures in the millimeter are consequently much higher than those obtained if the disk were isothermal.



However, the actual brightness temperatures may be very different if there is a vertically-dependent dust opacity, due to dust coagulation and settling. Moreover, they may be very different if a “dead zone” exists near the mid-plane, where viscous generation of energy is not occurring because there is not enough ionization to maintain the magneto rotational instability (MRI, Gammie 1996; Glassgold et al. 1997). The importance of this dead zone for planet formation is that inhibition of the MRI produces an increase of the density near the mid-plane (since matter cannot be transported inwards towards the star), favoring gravitational instabilities and potentially leading to planet formation.

## 5. Conclusions

The present evidence from disks around 1 to 10 Myr old stars indicates that dust growth and settling leading to planet formation and disk clearing happens fast and starts near the midplane in the few inner AU of the disk. Since the inner disk regions are optically thick to radiation shortwards of  $\sim 0.5$  mm, only ALMA in the highest resolution configuration, corresponding to  $0.01''$  or 1.4 AU at the closest star-forming regions, will allow us to reach the midplane of the planet-forming regions in the disks and study the processes that precede the formation of these bodies.

**Acknowledgments.** This work was supported in part by NASA grants NAGW 2306 and NAG5-4282.

## References

- Beckwith, S.V.W., Sargent, A.I., Chini, R. S., & Guesten, R. 1990, AJ, 99, 1024  
 Burrows, C.J. et al. 1996, ApJ, 473, 437  
 Cohen, M. & Kuhl, L.V. 1979, ApJS, 41, 743  
 D’Alessio, P., Cantó, J., Calvet, N., & Lizano, S. 1998, ApJ, 500, 411  
 D’Alessio, P., Cantó, J., Hartmann, L., Calvet, N., & Lizano, S. 1999a, ApJ  
 D’Alessio, P., Calvet, N., Hartmann, L., Cantó, J., & Lizano, S. 1999b, ApJ, (in press)  
 D’Alessio et al. 1999c, in preparation.  
 De La Reza, R., Torres, C.A., Quast, G., Castilho, B.V., Vieira, G.L. 1989 ApJ, 343, L61  
 Draine, B. T., & Lee, H. M. 1984, ApJ, 285,89  
 Dutrey, A., Guilloteau, S., Duvert, G., Prato, L., Simon, M., Schuster, K, & Menard, F. 1996, A & A, 309, 493  
 Gammie, C.F., 1996, ApJ, 457, 355  
 Glassgold, A.E., Najita, J., & Igea, J. 1997, 485, 920  
 Gomez, M., Hartmann, L., Kenyon, S.J., & Hewett, R. 1993, AJ, 105, 1927  
 Gullbring, E., Hartmann, L., Briceño, C., & Calvet, N., 1998, ApJ, 492, 323  
 Hartmann, L., Calvet, N., Gullbring, E., & D’Alessio, P. 1998, ApJ, 495, 385

- Herbig, G. 1978 in "Problems of Physics and Evolution of the Universe", ed. Mirzoyan, pub. Armenian Academy of Science
- Jayawardhana, R., Fisher, S., Hartmann, L., Telesco, C., Piña, R. & Fazio, G. 1998, *ApJL*, 503, L79
- Jayawardhana, R., Hartmann, L., Fazio, G., Fisher, S., Telesco, C., & Piña, R. 1999, *ApJ*, in press
- Kenyon, S.J., & Hartmann, L. 1987, *ApJ*, 323, 714
- Kenyon, S.J., & Hartmann, L. 1995, *ApJS*, 101, 117
- Koerner, D., Werner, M., Ressler, M., & Backman, D. 1998, *ApJL*, 503, L83
- Lynden-Bell, D., & Pringle, J. E. 1974, *MNRAS*, 168, 603
- McCaughrean, M.J., O'Dell, C.R. 1996, *AJ*, 111, 1977
- McCaughrean, M.J. et al. 1998, *ApJ*, 492, L157
- Meyer, M. R., Beckwith, S.V., Herbst, T.M., & Robberto, M. 1997, *ApJ*, 489, L173
- Miyake, K., & Nakagawa, Y. 1995, *ApJ*, 441, 361
- Podosek, F.A., & Cassen, P. 1994, *Meteoritics*, 29, 6
- Rucinski, S.M. 1985, *AJ*, 90, 2321
- Rucinski, S.M. & Krautter, J. 1983, *AA*, 121, 217
- Stapelfeldt, K.R., Krist, J.E., Ménard, F., Bouvier, J., Padgett, D.L., & Burrows, C.J. 1998, *ApJ*, 502, L65
- Schneider, G. et al. 1999, *ApJ*, 513, L127.
- Stauffer et al. 1999, in preparation
- Telesco, C. et al. 1999, in preparation
- Webb, R.A., Zuckerman, B., Platais, I., Patience, J., White, R.J., Schwartz, M.J. & McCarthy, C. 1999, *ApJ*, 512, L6